

13. Price, J., Droege, S. & Price, A. *The Summer Atlas of North American Birds* (Academic, San Diego, 1995).
14. Robbins, C. S., Bystrak, D. & Geissler, P. H. *The Breeding Bird Survey: Its First Fifteen Years, 1965–1979* (US Department of the Interior, Fish and Wildlife Service, Washington DC, 1986).
15. Sauer, J. R., Hines, J. E. & Fallon, J. *The North American Breeding Bird Survey, Results and Analysis 1966–2000 Version 2001.2* (USGS, Patuxent Wildlife Research Center, Laurel, Maryland, 2001); available at (<http://pwrctpr.er.usgs.gov/mp/bbs/DataFiles/>).
16. Pyke, C. R., Condit, R., Aguilar, S. & Lao, S. Floristic composition across a climatic gradient in a neotropical lowland forest. *J. Veg. Sci.* **12**, 553–566 (2001).
17. Burslem, D., Whitmore, T. & Brown, G. Short-term effects of cyclone impact and long-term recovery of tropical rain forest on Kolombangara, Solomon Islands. *J. Ecol.* **88**, 1063–1078 (2000).
18. Laurance, W., Ferreira, L., Rankin-De Merona, J. & Laurance, S. Rain forest fragmentation and the dynamics of Amazonian tree communities. *Ecology* **79**, 2032–2040 (1998).
19. Gaston, K. J. & Blackburn, T. M. *Pattern and Process in Macroecology* (Blackwell Science, Oxford, UK, 2000).
20. Tokeshi, M. Species abundance patterns and community structure. *Adv. Ecol. Res.* **24**, 111–186 (1993).
21. Pielou, E. C. *Mathematical Ecology* (John Wiley & Sons, New York, 1977).
22. Harte, J., Kinzig, A. P. & Green, J. Self-similarity in the distribution and abundance of species. *Science* **284**, 334–336 (1999).
23. Dewdney, A. K. A dynamical model of communities and a new species-abundance distribution. *Biol. Bull.* **198**, 152–165 (2000).
24. Kimura, M. *The Neutral Theory of Molecular Evolution* (Cambridge Univ. Press, Cambridge, UK, 1983).
25. McGill, B. J. Strong and weak tests of macroecological theory. *Oikos* (in the press).
26. Grimmett, G. R. & Stirzaker, D. R. *Probability and Random Processes* (Clarendon, Oxford, UK, 1992).
27. May, R. M. in *Ecology and Evolution of Communities* (eds Cody, M. L. & Diamond, J. M.) 81–120 (Belknap, Harvard Univ. Press, Cambridge, Massachusetts, 1975).
28. Hilborn, R. & Mangel, M. *The Ecological Detective: Confronting Models with Data* (eds Levin, S. A. & Horn, H. S.) (Princeton Univ. Press, Princeton, New Jersey, 1997).

Supplementary Information accompanies the paper on Nature's website (<http://www.nature.com/nature>).

Acknowledgements I thank the numerous volunteers who spent many hours collecting the BBS data, and the professionals at Patuxent Wildlife Research Center, who have put the data into an accessible, high-quality format, as well as those who collected and published the enormously valuable BCI data set. I also thank M. Rosenzweig, B. Enquist and the students in their laboratories for stimulating my thinking in this area. The National Science Foundation provided funding for this research. B. Walsh was a useful sounding board on statistics. Finally, I thank S. Marx, M. Weiser, D. Faulk and W. Turner for suggestions on an earlier draft of this paper, especially M. Weiser for his clarity on the importance of stopping rules, and S. Marx for greatly increasing the clarity of the paper.

Competing interests statement The author declares that he has no competing financial interests.

Correspondence and requests for materials should be addressed to the author (e-mail: mail@brianmcgill.org).

Ecological interference between fatal diseases

P. Rohani*, C. J. Green†, N. B. Mantilla-Beniers† & B. T. Grenfell†

* *Institute of Ecology, University of Georgia, Athens, Georgia 30602-2202, USA*

† *Zoology Department, University of Cambridge, Downing Street, Cambridge CB2 3EJ, UK*

An important issue in population biology is the dynamic interaction between pathogens. Interest has focused mainly on the indirect interaction of pathogen strains, mediated by cross immunity^{1–4}. However, a mechanism has recently been proposed for 'ecological interference' between pathogens through the removal of individuals from the susceptible pool after an acute infection. To explore this possibility, we have analysed and modelled historical measles and whooping cough records. Here we show that ecological interference is particularly strong when fatal infections permanently remove susceptibles. Disease interference has substantial dynamical consequences, making multi-annual outbreaks of different infections characteristically out of phase. So, when disease prevalence is high and is associated with significant mortality, it might be impossible to understand

epidemic patterns by studying pathogens in isolation. This new ecological null model has important consequences for understanding the multi-strain dynamics of pathogens such as dengue and echoviruses.

The possibility that epidemics of unrelated pathogens might interact has been raised in the classical epidemiological literature⁵, but has not been explained. Recently, a new mechanism has been proposed for negative ecological interference between pathogens through the temporary removal of susceptibles, arising from infection by a competing pathogen and the ensuing quarantine period⁶. Interference should be particularly apparent in the violent recurrent epidemics of strongly immunizing childhood infections such as measles and whooping cough. However, recent parallel records of the two infections in England and Wales show equivocal evidence for interference, partly because of the relatively low pathogenicity of the infections⁶. Here we test for interference in older data, collected when measles and whooping cough were significant killers⁵. Because a fatal infection involves the permanent removal of susceptibles, we would expect the imprint of interference to be particularly strong.

We begin by exploring the predictions of simple models, based on extensions of the classic one-disease seasonally forced SEIR (susceptible–exposed–infectious–removed) model^{7–9}, with two important biological refinements (see Methods). First, the model includes a convalescent class⁶, within which disease-induced deaths can occur; and second, we model the dynamics of two diseases simultaneously, categorizing hosts according to infection history relative to each disease. We are interested primarily in evaluating the dynamical impact of quarantine and disease-induced mortality on the community of pathogens. As with single-disease models, the dynamics of this system are determined largely by the recruitment rate of susceptibles (that is, the population birth rate^{7,8,10}; Fig. 1). Very low/high per-capita birth rates result in annual epidemics, with biennial dynamics observed for intermediate levels⁸. When there is a disease-related mortality rate, ρ , the window of biennial behaviour is progressively delayed, with the period-doubling bifurcation taking place at higher birth rates (Fig. 1a). This is because high mortality due to one infection in effect lowers the recruitment rate of susceptibles for the 'competing' disease. In general, the bifurcation structure of the model is dictated by the infection with the higher transmission rate—in this case, measles⁶. Whooping cough epidemics, which in isolation would be rigidly annual for all parameter combinations, now follow the same pattern as measles (Fig. 1b–d).

When epidemics are annual because of a low/high birth rate⁸, seasonal forcing causes strong positive correlation between infection outbreaks. However, given biennial epidemics, measles and whooping cough outbreaks are negatively correlated (out of phase)—much more so than if their dynamics were independent⁶. We use this negative correlation between disease dynamics as an indicator of potential interference in data.

We test for interference effects in case fatality reports for measles and whooping cough from Aberdeen (1883–1900) and from 15 European cities in the years before (1904–1914) and after (1922–1932) the First World War (Fig. 2). These data encompass large demographic heterogeneities, both spatial (between cities) and temporal (in the different eras). There were also systematic declines in the measles- and whooping-cough-induced death rates between periods before and after the war, which, along with the wide range of birth rates, provide an excellent opportunity to test the interference hypothesis in different regions of parameter space.

Children are typically affected by many more microparasitic infections than just measles and whooping cough (mumps, rubella and chickenpox within the childhood infections alone). However, we have focused on these two infections, because interference is likely to be most pronounced when diseases have very similar mean ages at infection, as dictated by their basic reproductive ratio, R_0 (ref. 7). Of potential childhood infections prevalent in the eras

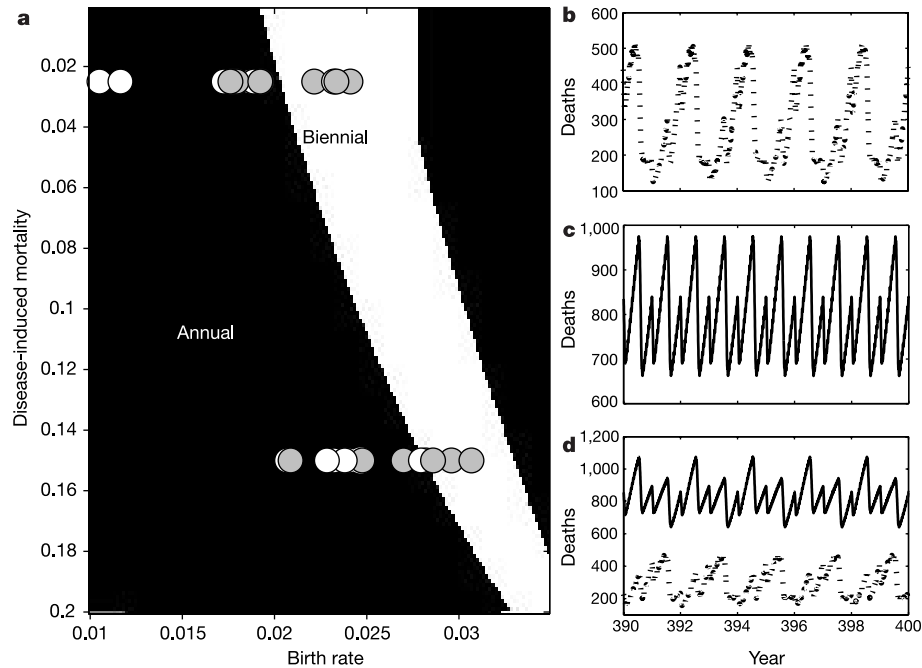


Figure 1 Analysis of the two-disease model dynamics. **a**, The bifurcation diagram illustrates the dynamics of the model as a function of the per-capita birth rate and the fraction of infecteds that suffer mortality. The black region highlights annual (and positively correlated) disease outbreaks; white regions identify biennial (negatively correlated) epidemics. The circles show the comparison with pre-war (mortality rate of 15%) and post-war (mortality rate of 2.5%) data. Negatively correlated data are

represented by grey circles; positive correlation is marked by a white circle. Panels **b–d** show time series for **b**, measles and **c**, whooping cough dynamics in single disease models compared with **d**, the two-disease model. The parameter values were: per-capita birth/death rate, 0.02; amplitude of seasonality, 0.3; incubation periods, 8 days; measles infectious period, 5 days; whooping cough infectious period, 14 days; measles convalescence period, 14 days; and whooping cough convalescence period, 21 days.

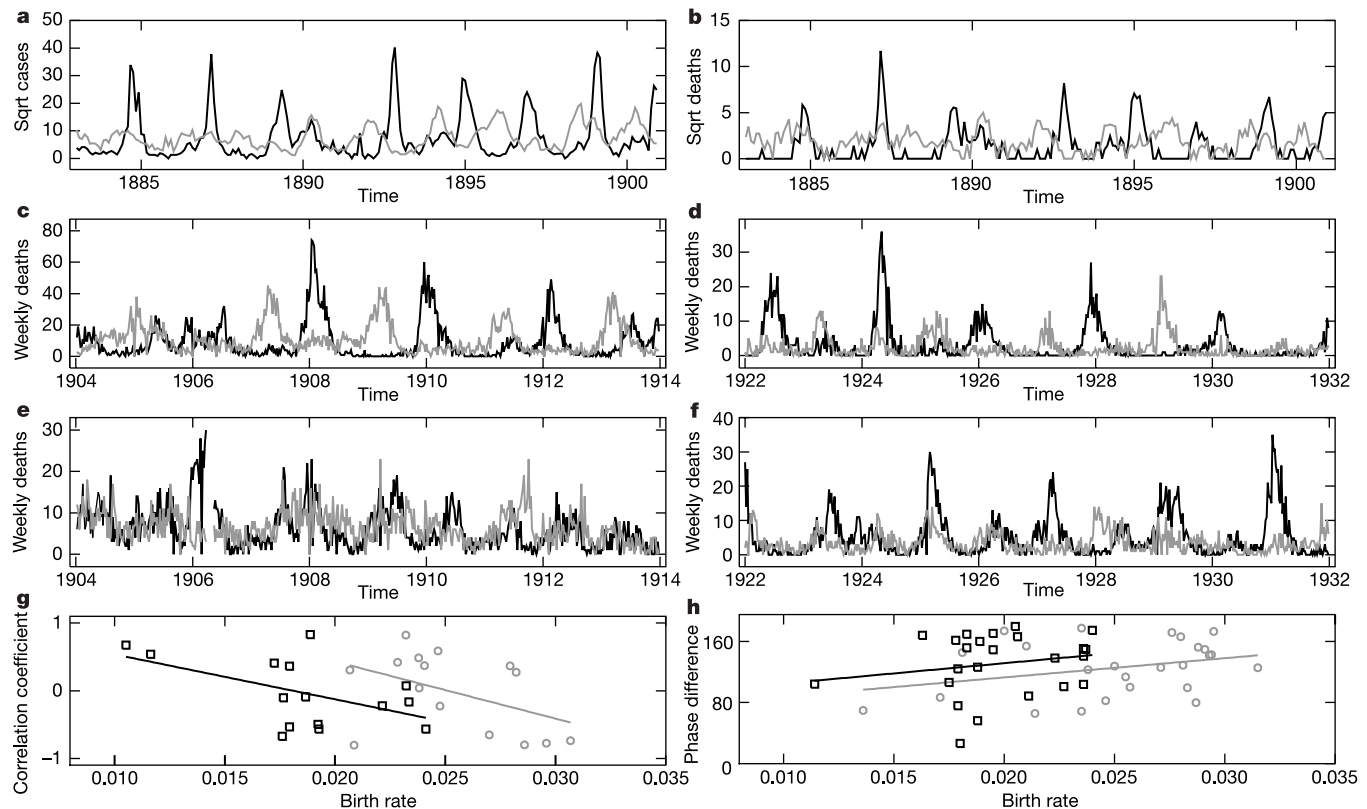


Figure 2 Weekly case fatality reports for measles (black) and whooping cough (grey) in five European cities. **a**, **b**, Case reports (**a**) and fatality (**b**) data for Aberdeen in the years 1882–1902. Sqrt, square root. **c–f** Weekly deaths due to these two infections from 1904 to 1914 (**c**, **e**), and from 1922 to 1932 (**d**, **f**). Data are shown for Birmingham (**c**,

Glasgow (**d**), Berlin (**e**) and Liverpool (**f**). **g**, **h**, Correlation coefficients (left) between measles and whooping cough deaths, and their associated epidemic phase differences (right) as a function of the per-capita birth rates (grey symbols/lines refer to the 1904–1914 era; black symbols/lines represent the period 1922–1932).

studied, measles and whooping cough have similar mean ages at infection (approximately 5 years¹¹); this suggests a potential for interference, which would be strengthened by the ‘cohort’ effect of school entry¹². By contrast, measles and whooping cough would be expected to interact much less with the other childhood diseases present, which tend to infect children at later ages (see table 2 in ref. 11). The potential for interference between less infectious diseases (with a greater spread in the age at infection), or infections conferring imperfect immunity, is an interesting area for future work.

The time series show typical infection dynamics for measles with mainly biennial cycles^{11–14}, although on occasion annual and triennial dynamics are also observed. The whooping cough deaths over the same periods tend to exhibit either annual or biennial epidemics. Examples of the observed dynamics from five cities can be seen in Fig. 2. Figure 2a, b clearly shows that, in Aberdeen, both case reports and case fatalities of measles and whooping cough are biennial and out of phase. This pattern is also seen in Birmingham (pre-war; Fig. 2c) and Glasgow (post-war; Fig. 2d), whereas in pre-war Berlin and post-war Liverpool, they are predominantly annual and in phase (Fig. 2e, f). We summarize the relationship between measles and whooping cough epidemics by plotting the mean per-capita birth rates against the correlation coefficient and the mean phase difference, respectively (Fig. 2g, h; see Methods). For both measures of synchrony, low birth rates are generally associated with annual (positively correlated) epidemics, whereas higher birth rates generally give rise to biennial (negatively correlated) dynamics. These results accord qualitatively with the predictions of the interference model.

For a more detailed comparison, we plot the mean annual per-capita birth rate for each city in each era against the estimated case

fatality rate (conservatively estimated to be around 15% in the pre-war era, dropping to 2.5% after the First World War). We have shaded each symbol according to the correlation coefficient between measles and whooping cough epidemics; white (grey) indicates a positive (negative) correlation. As can be seen in Fig. 1, there is a good qualitative agreement between model predictions and the data. Despite the uncertainty about historical parameter values, we see that cities with negative inter-disease correlations generally fall within the biennial asynchronous regions predicted by the model, whereas the annual positively correlated cities tend to lie within the annual synchronized areas. These results, together with those presented in Fig. 2g, h, suggest a significant interference interaction between the infections.

The results of this study have potentially profound implications for the analysis of multiple strain dynamics¹⁵. Cross immunity is often crucial, but, especially in the case of fatal infections, may be superimposed on the ‘ecological’ effects outlined here. To illustrate the issues, we developed a three-strain (SIR) extension of the model and explored correlations between strains as a function of their respective convalescence periods and fatality probability (Fig. 3). The model findings highlight strain epidemics that become strikingly out of phase as either the convalescence period or fatality probability increases. Although our model is intended to be quite generic, its conclusions are consistent with the observed epidemics of the serotypes of dengue fever¹⁶ and the three strains of echoviruses¹⁵. In these systems, strains are found to fluctuate erratically (without a characteristic period) and out of phase with each other. Until now, dengue dynamics have been assumed to be due to either environmental/ecological determinants of the mosquito vector *Aedes aegypti*^{17,18}, or complex immunological interactions between the different strains—so-called antibody-dependent enhancement¹⁹. This simple null model clearly shows that analyses of immunologically or environmentally driven strain dynamics need to take into account the underlying ecological dynamics of infections¹⁵. The construction of models for combined strain and interference dynamics is clearly a priority for future work.

More broadly, we believe that interference is a striking example of non-stationary disease community dynamics tuned by exogenous forces. It gives us an outstanding opportunity to study competitive dynamics on the scale of individuals, and their large-scale consequences. It also underlines the potential pitfalls of studying the components of any ecological system in isolation. □

Methods

The model

We modified the classic one-disease SEIR model⁷. Initially, individuals are susceptible to both diseases. On contracting one disease, they enter the exposed class, and have negligible probability of simultaneously contracting the second disease (owing to increased non-specific immunological activity)²⁰. After the incubation period is over, the individual becomes infectious and still has negligible probability of contracting the other disease. Typically, when clinical symptoms appear, children enter a convalescent phase and are removed from school. Usually, this would be followed by complete recovery and lifelong immunity (although this may not always be the case for whooping cough^{21,22}). However, depending on age and condition (typically nutritional status), infection may be fatal owing to complications (such as pneumonia and encephalitis). Surviving individuals are then susceptible to the second disease only. It is only after experiencing both diseases that the individual enters the fully recovered class. A mathematical description of the model is provided in Supplementary Tables 1 and 2. Variables have double subscripts to denote their infection history—hence, for example, S_{SR} refers to those who are susceptible to infection 1 (measles) but have recovered from infection 2 (whooping cough).

To mimic the aggregation of children in schools, the model incorporates a seasonally varying contact rate—‘term-time forcing’²³. For infection i , the contact parameter $\beta_i(t)$ depends on the time of year, being high on school days and low on other days. The parameters b_{0i} and b_1 are the disease-specific basic transmission rate and the seasonal amplitude, respectively.

$$\beta_i(t) = b_{0i}(1 \pm b_1)$$

European data

The data we present were published by the Registrar General’s Weekly Returns. The correlation between case fatality data and infection levels is not well established. However, Butler presented data for London and Willesden in which there is a clear linear

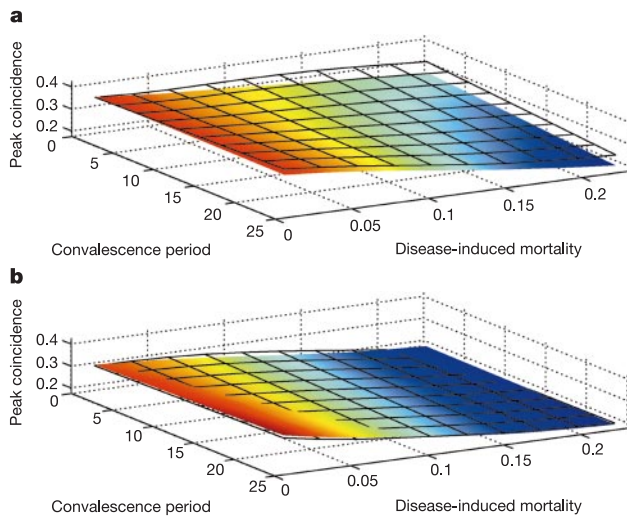


Figure 3 Temporal synchrony of strains, produced by a stochastic three-disease model. In **a**, $R_0 = 5$; in **b**, $R_0 = 10$. For any specific parameter combination, we estimated the pair-wise peak coincidence likelihood from a 250-year model time series, averaged them and fitted a spline (coloured surface). Peak coincidence, P , for a pair of time series is estimated by calculating the number of times they simultaneously peak (M) divided by the number of peaks, $\max[M_i, M_j]$, where M_i is the number of peaks for time-series i (ref. 30). To estimate confidence intervals, we randomized the phases of the time series 1,000 times and estimated P . The transparent surface shows a spline fitted to the 5th percentile of the bootstrapped values of P . As ρ (disease-induced mortality) or $1/\delta$ (convalescence period) increases, there is a decline in the peak coincidence levels, and strain epidemics become significantly out of phase (the coloured surface lies beneath the transparent one). Model parameters were per-capita birth/death rate, 0.02; amplitude of seasonality, 0.3; incubation plus infectious periods, 8, 9 and 10 days, respectively, for the three strains. Stochasticity was introduced into the model by making the transmission rate variable $\sim b_{0i} \times N(1, 0.05)$. This was estimated daily for each strain.

correspondence between case reports and fatality data. These data also establish that mortality rates are not affected by epidemic phase²⁴. Further confirmation of these results is provided by an analysis of the Aberdeen data (N.B.M.-B., P.R. and B.T.G., manuscript in preparation). Concerning infection-induced mortality rates, classic work by Butler²⁴, Bartlett²⁵, Creighton⁵ and others indicates significant mortality due to measles and whooping cough during these periods. Estimates of case fatality rates for measles vary widely, from 1–2% in the post-war era up to 46% pre-war^{14,26,27}, whereas estimates for whooping cough are in the 3–15% range²⁴.

Data analysis

These time series contain a substantial annual component and are further complicated by increasing population sizes over the two periods examined. Hence, analyses of the relationship between measles and whooping cough outbreaks were carried out on de-trended data. We used three separate methods. First, Pearson correlation coefficients were estimated for data aggregated over each epidemic year (October to October). Second, we carried out a linear regression of annual counts of measles against whooping cough and used the slope as a measure of synchrony. The results of this technique were qualitatively identical to those of the Pearson correlation, so we present only those. Finally, we also used Wavelet spectra to explore phase differences between filtered time series^{28,29}. Further information can be found in the Supplementary Information.

Bifurcation analysis

The bifurcation diagram was prepared by solving the system of ordinary differential equations (ODEs) for each parameter combination and characterizing the dynamics after a 190-year transient period was ignored. We used wrap-around initial conditions (whereby the final conditions for a run were used as the initial conditions for the next run). In the regions where the birth rates are relatively small, more than one attractor can coexist, although annual dynamics have the largest basin⁸. Note that in model dynamics, for some very restricted choice of initial conditions, it is possible to observe biennial dynamics that are in phase. However, work in progress has shown that infection dynamics become out of phase when stochasticity is introduced into the model, consistent with the findings of Kamo and Sasaki¹⁵.

Received 9 January; accepted 25 February 2003; doi:10.1038/nature01542.

- Gog, J. R. & Swinton, J. A. A status-based approach to multiple strain dynamics. *J. Math. Biol.* **44**, 169–184 (2002).
- Gupta, S., Ferguson, N. M. & Anderson, R. M. Chaos, persistence and evolution of strain structure in antigenically diverse infectious agents. *Science* **280**, 912–915 (1998).
- Gomes, M. G. M., Medley, G. F. & Nokes, D. J. On the determinants of population structure in antigenically diverse pathogens. *Proc. R. Soc. Lond. B* **269**, 227–233 (2002).
- Dietz, K. Epidemiologic interference of virus populations. *J. Math. Biol.* **8**, 291–300 (1979).
- Creighton, C. *A History of Epidemics in Britain* (Cambridge Univ. Press, Cambridge, 1894).
- Rohani, P., Earn, D. J. D., Finkenstädt, B. F. & Grenfell, B. T. Population dynamic interference among childhood diseases. *Proc. R. Soc. Lond. B* **265**, 2033–2041 (1998).
- Anderson, R. M. & May, R. M. *Infectious Diseases of Humans: Dynamics and Control* (Oxford Univ. Press, Oxford, 1991).
- Earn, D. J. D., Rohani, P., Bolker, B. M. & Grenfell, B. T. A simple model for complex dynamical transitions in epidemics. *Science* **287**, 667–670 (2000).
- Rand, D. A. & Wilson, H. B. Chaotic stochasticity: a ubiquitous source of unpredictability in epidemics. *Proc. R. Soc. Lond. B* **246**, 179–184 (1991).
- McLean, A. & Anderson, R. Measles in developing countries part I. Epidemiological parameters and patterns. *Epidemiol. Infect.* **100**, 111–133 (1988).
- Anderson, R. M. & May, R. M. Directly transmitted infectious diseases: control by vaccination. *Science* **215**, 1053–1060 (1982).
- Schenzle, D. An age-structured model of pre- and post-vaccination measles transmission. *IMA J. Math. Appl. Med. Biol.* **1**, 169–191 (1984).
- Rohani, P., Earn, D. J. D. & Grenfell, B. T. Opposite patterns of synchrony in sympatric disease metapopulations. *Science* **286**, 968–971 (1999).
- Butler, W. Measles. *Proc. R. Soc. Med.* **6**, 120–153 (1913).
- Kamo, M. & Sasaki, A. The effects of cross-immunity and seasonal forcing in a multi-strain epidemic model. *Physica D* **165**, 228–241 (2002).
- Wenjie, W. Control of dengue/dengue haemorrhagic fever in china. *Dengue Bull.* **21** (<http://w3.whosea.org/DengueBulletin21/ch3f.htm>) (1997).
- Focks, D. A., Brenner, R. J., Hayes, J. & Daniels, E. Transmission thresholds for dengue in terms of *Aedes aegypti* pupae per person with discussion of their utility in source. *Am. J. Trop. Med. Hyg.* **62**, 11–18 (2000).
- Hales, S., de Wet, N., Maindonald, J. & Woodward, A. Potential effect of population and climate changes on global distribution of dengue fever: an empirical model. *Lancet* **360**, 830–834 (2002).
- Kurane, I., Mady, B. J. & Ennis, F. A. Antibody-dependent enhancement of dengue virus infection. *Rev. Med. Virol.* **1**, 211–222 (1991).
- Behrman, R. E. & Kliegman, R. M. *Nelson Essentials of Pediatrics* (Saunders, Philadelphia, 1998).
- Cherry, J. D. Pertussis in adults. *Ann. Intern. Med.* **128**, 64–66 (1998).
- Miller, E. & Gay, N. Epidemiological determinants of pertussis. *Dev. Biol. Stand.* **89**, 15–23 (1997).
- Keeling, M. J., Rohani, P. & Grenfell, B. T. Seasonally forced disease dynamics explored as switching between attractors. *Physica D* **148**, 317–335 (2001).
- Butler, W. Whooping cough and measles. *Proc. R. Soc. Med.* **40**, 384–398 (1947).
- Bartlett, M. S. Measles periodicity and community size. *J. R. Stat. Soc.* **1**, 48–59 (1957).
- Soper, H. E. The interpretation of periodicity in disease prevalence. *J. R. Stat. Soc.* **92**, 34–73 (1929).
- Linnert, L. *A statistical report on measles notifications in Manchester, 1917–1951*. (Department of Mathematical Statistics, Manchester, UK, 1954).
- Grenfell, B. T., Bjornstad, O. N. & Kappey, J. Travelling waves and spatial hierarchies in measles epidemics. *Nature* **414**, 716–723 (2001).
- Torrence, C. & Compo, G. P. A practical guide to wavelet analysis. *Bull. Am. Meteorol. Soc.* **79**, 61–78 (1998).

30. Buonaccorsi, J. P., Elkington, J. S., Evans, S. R. & Liebold, A. M. Measuring and testing for spatial synchrony. *Ecology* **82**, 1668–1679 (2001).

Supplementary Information accompanies the paper on *Nature's* website (<http://www.nature.com/nature>).

Acknowledgements We thank O. Bjornstad, M. Boots, D. Gubler and H. Wearing for comments on this manuscript.

Competing interests statement The authors declare that they have no competing financial interests.

Correspondence and requests for materials should be addressed to P.R. (e-mail: rohani@uga.edu).

Unique physiological and pathogenic features of *Leptospira interrogans* revealed by whole-genome sequencing

Shuang-Xi Ren*†‡, Gang Fu*§‡, Xiu-Gao Jiang||‡, Rong Zeng†‡, You-Gang Miao†, Hai Xu†, Yi-Xuan Zhang†, Hui Xiong§, Gang Lu*, Ling-Feng Lu*, Hong-Quan Jiang*§, Jia Jia*, Yue-Feng Tu*, Ju-Xing Jiang¶, Wen-Yi Gu*, Yue-Qing Zhang*#, Zhen Cai*, Hai-Hui Sheng*, Hai-Feng Yin*, Yi Zhang*, Gen-Feng Zhu*, Ma Wan||, Hong-Lei Huang||, Zhen Qian*, Sheng-Yue Wang*, Wei Ma†, Zhi-Jian Yao¶, Yan Shen¶, Bo-Qin Qiang¶, Qi-Chang Xia†, Xiao-Kui Guo§, Antoine Danchin☆, Isabelle Saint Girons**, Ronald L. Somerville††, Yu-Mei Wen#, Man-Hua Shi||‡‡, Zhu Chen*§, Jian-Guo Xu|| & Guo-Ping Zhao*†

* Chinese National Human Genome Center at Shanghai (CHGCS), 250 Bi Bo Road, Zhang Jiang High Tech Park, Shanghai 201203, China

† Bioinformation Center/Institute of Biochemistry and Cell Biology/Institute of Plant Physiology and Ecology/Research Center of Biotechnology, Shanghai Institutes for Biological Sciences, Chinese Academy of Sciences, 320 Yue Yang Road, Shanghai 200031, China

§ Rui Jin Hospital/Department of Microbiology and Parasitology, Shanghai Second Medical University, 280 Chongqingnan Road, Shanghai 200025, China || National Institute for Communicable Disease Control and Prevention, Chinese Center for Disease Control and Prevention (ICDC, China CDC), P.O. Box 5, Changping, Beijing 102206, China

¶ Chinese National Human Genome Center, Beijing, 707 North Yongchang Road, Yi Zhuang High Tech Park, Beijing 100170, China

Department of Molecular Virology, Medical Center, Fudan University, 138 Yi Xue Yuan Road, Shanghai 200032, China

☆ HKU-Pasteur Research Centre, 8, Sassoon Road, Hong Kong, China

** Unité de Bactériologie Moléculaire et Médicale, Institut Pasteur, 25, rue du docteur Roux, 75724 Paris Cedex 15, France

†† Department of Biochemistry, Purdue University, West Lafayette, Indiana 47907, USA

‡ These authors contributed equally to this work
‡‡ Deceased

Leptospirosis is a widely spread disease of global concern. Infection causes flu-like episodes with frequent severe renal and hepatic damage, such as haemorrhage and jaundice. In more severe cases, massive pulmonary haemorrhages, including fatal sudden haemoptysis, can occur¹. Here we report the complete genomic sequence of a representative virulent serovar type strain (Lai)² of *Leptospira interrogans* serogroup Icterohaemorrhagiae consisting of a 4.33-megabase large chromosome and a 359-kilobase small chromosome, with a total of 4,768 predicted genes. In terms of the genetic determinants of physiological characteristics, the facultatively parasitic *L. interrogans* differs